

Autodissociation of doubly charged water molecules

S. W. J. Scully, J. A. Wyer, V. Senthil, and M. B. Shah

Department of Physics and Astronomy, Queen's University Belfast, Belfast BT7 1NN, United Kingdom

E. C. Montenegro

Instituto de Física, Universidade Federal do Rio de Janeiro, Cx. Postal 68528, Rio de Janeiro, RJ 21941-972, Brazil

(Received 11 November 2005; published 14 April 2006)

The electron impact dissociative double-ionization cross sections for H_2O between 45 and 1500 eV have been measured using time of flight mass spectrometry. The energy dependence of the $\text{H}^+ + \text{OH}^+$ and $\text{H}^+ + \text{O}^+$ ion pair production cross sections indicate that Auger-like autoionization following a vacancy in the $2a_1$ molecular orbital is the main double ionization channel at high velocities. In contrast to expectation, these findings show that dissociation through the H_2O^{2+} precursor state is a significant process at high collision energies. Knowledge of this process is vital as it has a direct affect on the production of important molecular species, such as H_2 , during water radiolysis. Branching ratios of the various fragments produced following both autoionization and double ionization have also been obtained.

DOI: [10.1103/PhysRevA.73.040701](https://doi.org/10.1103/PhysRevA.73.040701)

PACS number(s): 34.80.Gs, 34.80.Ht

The nature and composition of the earth's biosphere in the early stages of its history were highly influential to the development of life. The predominance of a reducing or oxidizing primordial atmosphere remains an open question. As does the understanding of how the transition to the current oxidizing atmosphere occurred. In any event, before the appearance of photosynthesis, abiogenic energy sources necessary to power the synthesis of hydrocarbons must be invoked. This energy source could have come from the H_2 and O_2 formed from the fragments produced during water radiolysis. This radiolysis was most likely caused by the products of nuclear processes [1,2]. Natural radioactive decay of heavy nuclei and ^{40}K was much more abundant 4000 Ma ago [2,3] and these eject energetic fission products, such as α particles, γ rays, and fast electrons. Computer simulations show that the amount of H_2 generated by water radiolysis from ^{40}K is comparable to those released by volcanic activity, 3800 Ma ago [2].

H_2 and O_2 produced by water radiolysis were recently suggested as markers of the presence of U mineralization [4]. In these sites, the presence of both gases can have a profound influence in the reproduction rate of living organisms. Abiogenic synthesis of energy rich compounds such as CH_4 , NH_3 , and H_2 , driven by water radiolysis were recently found in 3.1 km deep ground water, supporting microbial life at this depth [5]. The high concentrations of H_2 found probably inhibit the proliferation of micro-organisms, which were found in scarce communities [5]. In the same way, the concentrations of H_2 observed in ground water of the precambrian shield are also consistent with radiolysis of water and are well above those required to support H_2 -requiring micro-organisms [6].

Much of the present status of knowledge about the environmental changes caused by the fragmentation of water by radiation, such as above, or in other equally important cases, such as tumor treatment or corrosion in nuclear reactors, have been obtained with the aid of measurements in the gas phase together with the use of Monte Carlo simulations. In all of these scenarios, and for all types of impinging par-

ticles, fast electrons are often produced and these play a key role in the determination of the amount and the quality of the water fragmentation. These electrons also play an important role in water's postcollisional chemistry and in the products released.

It is generally accepted that radiolysis by low linear energy transfer (LET) particles, such as electrons, is well understood, and much of the recent effort has concentrated on the study of high LET heavy ions [7–10]. In the absence of dissociative branching ratios following double ionization of water by electrons, the present well understood status relies on the assumption that doubly charged water is unimportant and a negligible fraction of the whole ionization process. However, the H_2 and O_2 formation in liquid water cannot be fully understood without considering double ionization processes. Double ionization produces the main precursors for H_2 and O_2 formation, which are a pair of hydrated electrons *at the same site* [11,12] and O atoms, respectively [10]. Thus, any attempt to properly understand and calculate H_2 and O_2 production from liquid water by an electron impact requires a number of cross sections, such as those for $\text{H}^+ + \text{OH}^+$ and $\text{H}^+ + \text{O}^+$ ion pair productions. These have not been measured previously. More knowledge of the role played by autoionization in doubly charged water ions contributing to the above pathways is also required. In this Rapid Communication, these questions are addressed by reporting the measurements of the fragmentation patterns of doubly ionized water.

The main features of the crossed beam experimental arrangement used in the present work have been described previously [13–15]. Briefly, the interaction region where an electron beam and a target beam cross at right angles to one another is surrounded by two high transparency grids mounted on two conical electrodes inside a high vacuum chamber. The target beam was 4 mm in diameter and was formed by effusing gas through a 2 mm diameter tube inside a separate differentially pumped chamber. The electron beam was pulsed with a 65 ns pulse width and a 10^5 Hz repetition rate. The ions extracted after electron impact were guided

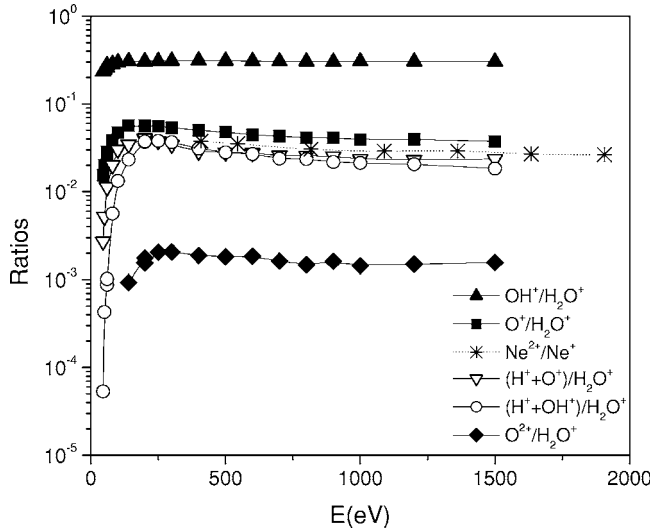


FIG. 1. Cross section ratios relative to H_2O^+ . Also shown are the $\text{Ne}^{2+}/\text{Ne}^+$ ratios obtained with equivelocity protons from Ref. [17] for comparison. The ratios are approximately independent of the impinging energy for $E > 200$ eV.

through a focusing lens system into a field free drift region of about 10 cm in length and were subsequently detected by a stack of three multichannel plates (MCP).

A time to amplitude converter (TAC) operated with start pulses from the extraction pulse generator and stop pulses from the MCP detector provided time of flight product ion spectra. Spectra were obtained for electron beam energies from 45 to 1500 eV. In addition to these measurements of the partial ionization yields, the signal recording system was modified so that it was also possible to measure spectra for the production of a H^+ or H_2^+ ion in coincidence with other fragment ion species. In this arrangement a second TAC was gated by the output of the first TAC, set to a window on the H^+ or H_2^+ ion peak. Therefore, the second TAC only operated when a H^+ or H_2^+ ion was detected on the first TAC. The start and stop pulses to the second TAC were the same as for the first but were suitably delayed to make allowance for the signal processing time of the gate signal.

The system was calibrated using the known electron impact cross sections for CH_4 gas. The measured signals for each product ion and coincidence ion species were normalized to the CH_4 absolute total cross sections reported by Straub *et al.* [16]. The efficiency of the TOF detector was determined by measuring the signal at its output and comparing this with the intensity of the signal current measured on the first plate of the MCP. The electron beam intensity was increased by four orders of magnitude to make this measurement feasible. The efficiency of the detector was thereby determined to be 0.17 ± 0.02 . The calculated normalization factor was then used to determine cross section values for the ions produced in coincidence with H^+ ions.

Figure 1 shows the measured cross sections ratios of the H_2O electron impact fragmentation products, following single or double ionization, with respect to H_2O^+ production. The $\text{Ne}^{2+}/\text{Ne}^+$ ratio, for equivelocity proton impact [17] is also shown. The H^++H^+ channel could not be measured in our arrangement because it is embedded in the total H^+ chan-

nel. All measured ratios tend to constant values at high velocities, including those which are explicitly related to double-ionization channels such as H^++O^+ , H^++OH^+ , O^{2+} , and Ne^{2+} . This is the behavior expected from autoionization.

The Ne case was studied in Refs. [17,18] where it was shown that the constant ratio, at high velocities, is indeed due to a postcollisional Auger-like autoionization following a vacancy produced by a single ionization.

Double ionized water (H_2O^{2+}) is unstable. This instability produces a dissociation pattern which results from several possible combinations of losing two electrons from the $2a_1$ (32.62), $1b_2$ (18.78), $3a_1$ (14.84), and $1b_1$ (12.60) levels—the numbers between parentheses are the binding energies in eV [19]. Whatever the levels involved, collisional double-ionization gives an energy dependence for the cross sections which is essentially the same for all levels [20]. The energy dependance for double- to single-ionization ratios tend to constant values at high impact velocities. These constant ratios indicate that autoionization is the main process involving two-electron ejection for swift projectiles. The main thrust of the present work is to address the branching ratios for the dissociative autoionization pattern of water. This is the first time such a study has been undertaken to the best of our knowledge.

In the following analysis it is assumed that two-electron emission comes from (i) the single ionization of $2a_1$ level (σ_{2a_1}) followed by Auger-like decay (defined by coefficients; A_2, A_3, A_4, A_5) (ii) double ionization involving the four above-mentioned molecular orbitals (σ_{2i}), and that, in a competition to autoionization, a single vacancy in the $2a_1$ orbital can decay either by O^+ (S_1) or H^+ (S_4) emission, as suggested by Refs. [7,21]. The corresponding cross sections are given by

$$\sigma_{\text{O}^+} = (S_1 + A_3)\sigma_{2a_1} + B_3\sigma_{2i}, \quad (1)$$

$$\sigma_{\text{OH}^++\text{H}^+} = A_2\sigma_{2a_1} + B_2\sigma_{2i}, \quad (2)$$

$$\sigma_{\text{O}^++\text{H}^+} = A_3\sigma_{2a_1} + B_3\sigma_{2i}, \quad (3)$$

$$\sigma_{\text{H}^++\text{H}^+} = A_4\sigma_{2a_1} + B_4\sigma_{2i}, \quad (4)$$

$$\sigma_{\text{O}^{2+}} = A_5\sigma_{2a_1} + B_5\sigma_{2i}, \quad (5)$$

$$\sigma_{\text{H}^++\text{neutrals}} = S_4\sigma_{2a_1}. \quad (6)$$

Equations (1)–(3) can be combined to give

$$\frac{\sigma_{\text{OH}^++\text{H}^+}}{\sigma_{\text{O}^++\text{H}^+}} = \alpha \frac{\sigma_{\text{O}^+}}{\sigma_{\text{O}^++\text{H}^+}} + \beta, \quad (7)$$

where it is straightforward to show that $A_2 = \alpha S_1 + (\alpha + \beta)A_3$ and $B_2 = (\alpha + \beta)B_3$. In the case where $A_2 = A_3 = 0$, i.e., if there is no autoionization, then $\alpha = 0$ and $\beta = B_2/B_3$. Thus, the slope of Eq. (7) is directly associated to the presence of an autoionization process. Figure 2 shows the cross section measurements, plotted according to Eq. (7), for energies from 60 to 1500 eV. The coalescence of the data in a straight

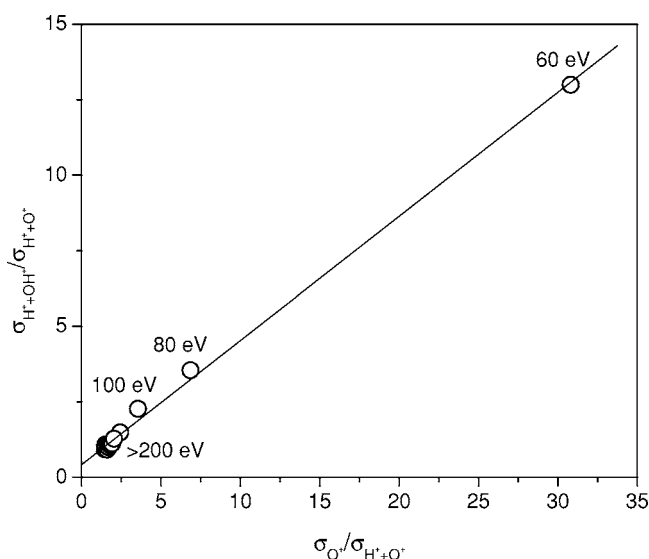


FIG. 2. Correlation between $\sigma_{OH^++H^+}/\sigma_{O^++H^+}$ and $\sigma_{O^+}/\sigma_{O^++H^+}$, according to Eq. (7). The slope of this line is related to an Auger-like autoionization following a vacancy in the $2a_1$ molecular orbital of water.

line, with $\alpha=0.412$ and $\beta=0.418$, indicates that autoionization is present as a postcollisional decay for all electron energies above ≈ 60 eV.

The determination of the coefficients appearing in Eqs. (1)–(6) can be obtained using the relations between A_2 , A_3 , B_2 , B_3 , α and β mentioned above and the constraints, $S_1 + S_4 + A_2 + A_3 + A_4 + A_5 = 1$ and $B_2 + B_3 + B_4 + B_5 = 1$, together with a best-fit to the measured cross sections σ_{O^+} , $\sigma_{OH^++H^+}$, $\sigma_{O^++H^+}$, and $\sigma_{O^{2+}}$. To this end, σ_{2a_1} was calculated using the procedure of Ref. [22] and σ_{2i} through the scaling [20] of the ratio, R , between double and single ionization of Ne by swift protons, as given in Ref. [23], and using the known ionization energies for water. Thus, $\sigma_{2i} = R \sigma_{total}$, where the total ionization of water, σ_{total} , was also calculated according to Ref. [22]. Furthermore, as $\sigma_{H^++H^+}$ was not measured, the high-velocity ratio $\sigma_{H^++H^+}/\sigma_{O^++H^+} = 4.2 \sim A_4/A_3$ given by Ref. [7] was used to determine A_4 . This procedure gives $S_1 = 0.15$, $S_4 = 0.176$, $A_2 = 0.145$, $A_3 = 0.1$, $A_4 = 0.42$, $A_5 = 0.009$, $B_2 = 0.307$, $B_3 = 0.37$, $B_4 = 0.305$, and $B_5 = 0.018$. Due to threshold effects with electron impact, the proton scaling for σ_{2i} is only valid for energies above 200 eV.

The relative contributions of the collisional double ionization and autoionization for $\sigma_{OH^++H^+}$ and $\sigma_{O^{2+}}$ are shown in Fig. 3. It is clear that the contributions from $2a_1$ single ionization, followed by Auger decay, dominate at high energies and are not insignificant at low energies. Direct double ionization is important at low energies, however the shape for the contributions of direct double ionization, derived from the model, do not agree with the experiment at low energies as a result of threshold behavior.

The present measurements for $\sigma_{H_2O^+}$ and the theoretical σ_{total} , together with those of Rao *et al.* are shown in Fig. 4. Absolute cross sections for the various fragmentation products can be obtained from this data and those shown in Fig. 1. The present analysis of double ionization provides the total cross section for the two-electron production, which is

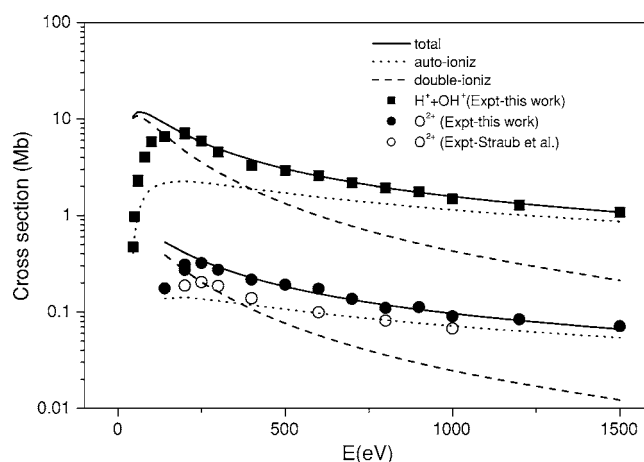


FIG. 3. Cross sections for OH^++H^+ and O^{2+} production. Closed squares and closed circles, this work; open circles, Ref. [24]. Dashed lines, contributions from double ionization; dotted lines, contributions from autoionization; full lines, sum of both contributions.

shown in Fig. 4, and which is calculated using

$$\sigma_{2e} = (A_2 + A_3 + A_4)\sigma_{2a_1} + (B_2 + B_3 + B_4)\sigma_{2i}. \quad (8)$$

From Fig. 4 it is clear that, due to autoionization, the processes in which doubly charged water is a precursor are much more important at high energies than what would be expected just from direct double ionization. Similar double-to-single-ionization ratios were obtained for molecules such as HCl [26], N_2 , and O_2 [27]. For water there is no previous direct measurement for double ionization, and inferences taken from noncoincidence measurements can lead to underestimated values for the double-ionization channel [28]. As

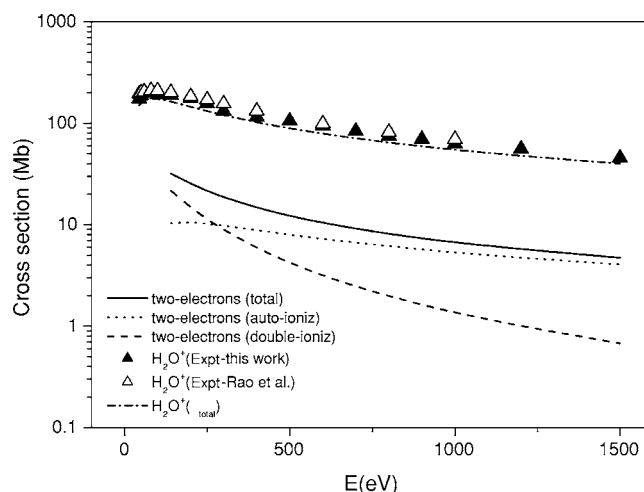


FIG. 4. Cross sections for the H_2O^+ production. Closed triangles, this work; open triangles, Ref. [25]. Dashed-dotted line, σ_{total} (calculated total ionization cross section). Also shown are modeled cross sections for the two electron production. Dashed lines, contributions from direct double-ionization; dotted lines, contributions from auto-ionization; full lines, sum of both contributions.

noted above the previous lack of information concerning dissociative double ionization has meant that it has not been properly included in the modeling of water radiolysis [7,11]. The inclusion of these cross sections is required for a full understanding of H₂ and O₂ production, via energetic electrons. Proximity is an essential parameter in producing these molecular species after water radiolysis. As the density of products in the track gets larger, by the use of heavy particles, for example, the amount of ionized molecular species increases [11]. Double ionization, on the other hand, produces several molecular ions *at the same site* and allows production of close lying molecular species even for low-LET radiation.

The main reactions leading to H₂ production involve hydrated electrons (e_{aq}⁻), which are produced by thermalization after ionization in about 240 fs [12]. According to Ref. [11], H₂ comes mostly from two reactions: e_{aq}⁻+e_{aq}⁻→H₂+2OH⁻ or H+H→H₂. This last reaction can be accomplished

through the chain reaction e_{aq}⁻+H⁺→H followed by H+H→H₂. *All these ingredients are present in the double-ionization processes* discussed here. Indeed, cross sections (2)–(4) measure the simultaneous production of H⁺ and two electrons at the same site. The main point of the present work is to show that, because of autoionization, dissociative double ionization is important for essentially all electron energies. For example, σ_{2e} is larger than 10% of σ_{H₂O⁺} for all energies studied in this work, with this proportion remaining approximately constant for E>500 eV. These processes are clearly more significant than previously assumed.

The support of the UK Engineering and Physical Science Research Council is gratefully acknowledged. E.C.M. would like to thank the International Research Center for Experimental Physics at Queen's University of Belfast for providing him with support. E.C.M would like also to acknowledge support from Brazilian Agencies CNPq and FAPERJ.

-
- [1] V. P. Shilov and A. V. Gogolev, *Radioact. Radiochem.* **44**, 209 (2002).
- [2] I. G. Draganić, *Radiat. Phys. Chem.* **72**, 181 (2005).
- [3] F. G.-Lafaye and F. Weber, *Precambrian Res.* **120**, 81 (2003).
- [4] D. Derome *et al.*, *J. Geochem. Exploration* **80**, 259 (2003).
- [5] T. L. Kieft *et al.*, *Geomicrobiol. J.* **22**, 325 (2005).
- [6] L.-H. Lin *et al.*, *Geochim. Cosmochim. Acta* **69**, 893 (2005).
- [7] G. H. Olivera *et al.*, *Phys. Med. Biol.* **43**, 2347 (1998).
- [8] B. Coupier *et al.*, *Eur. Phys. J. B* **20**, 459 (2002).
- [9] H. Luna and E. C. Montenegro, *Phys. Rev. Lett.* **94**, 043201 (2005).
- [10] B. Gervais, M. Beuve, G. H. Olivera, M. E. Galassi, and R. D. Rivarola, *Chem. Phys. Lett.* **410**, 330 (2005).
- [11] Y. Frongillo *et al.*, *Radiat. Phys. Chem.* **51**, 245 (1998).
- [12] J. A. LaVerne and S. M. Pimblott, *J. Phys. Chem.* **104**, 9820 (2000).
- [13] M. B. Shah, D. S. Elliott, and H. B. Gilbody, *J. Phys. B* **20**, 3501 (1987).
- [14] P. McCallion, M. B. Shah, and H. B. Gilbody, *J. Phys. B* **25**, 1061 (1992).
- [15] S. W. J. Scully *et al.*, *Phys. Rev. A* **72**, 030701(R) (2005).
- [16] H. C. Straub, D. Lin, B. G. Lindsay, K. A. Smith, and R. F. Stebbings, *J. Chem. Phys.* **106**, 4430 (1997).
- [17] E. G. Cavalcanti, G. M. Sigaud, E. C. Montenegro, M. M. Sant'Anna, and H. Schmidt-Böcking, *J. Phys. B* **35**, 3937 (2002).
- [18] T. Spranger and T. Kirchner, *J. Phys. B* **37**, 4159 (2004).
- [19] B. Winter *et al.*, *J. Phys. Chem. A* **108**, 2625 (2004).
- [20] M. M. Sant'Anna, E. C. Montenegro, and J. H. McGuire, *Phys. Rev. A* **58**, 2148 (1998).
- [21] K. H. Tan, C. E. Brion, Ph. E. Van der Leeuw, and M. J. van der Wiel, *Chem. Phys.* **29**, 299 (1978).
- [22] W. Hwang, Y.-K. Kim, and M. E. Rudd, *J. Chem. Phys.* **104**, 2956 (1996).
- [23] H. Luna, E. G. Cavalcanti, J. Nickles, G. M. Sigaud, and E. C. Montenegro, *J. Phys. B* **36**, 4717 (2003).
- [24] H. C. Straub, B. G. Lindsay, K. A. Smith, and R. F. Stebbings, *J. Chem. Phys.* **108**, 109 (1998).
- [25] M. V. Rao, I. Iga, and S. K. Srivastava, *J. Geophys. Res.* **100**, 26421 (1995).
- [26] S. Harper, P. Calandra, and S. D. Price, *Phys. Chem. Chem. Phys.* **3**, 741 (2001).
- [27] C. Tian and C. R. Vidal, *J. Phys. B* **31**, 5369 (1998).
- [28] F. Frémont *et al.*, *Phys. Rev. A* **72**, 042702 (2005).